




Article

Prunetin 4'-O-Phosphate, a Novel Compound, in RAW 264.7 Macrophages Exerts Anti-Inflammatory Activity via Suppression of MAP Kinases and the NF κ B Pathway

Tae-Jin Park ¹, Hye Hyun Hong ¹, Min-Seon Kim ², Jin-Soo Park ², Won-Jae Chi ³ and Seung-Young Kim ^{1,*}

¹ Department of Pharmaceutical Engineering & Biotechnology, Sunmoon University, Asan 31460, Korea; bark.taejin@gmail.com (T.-J.P.); kongjjo123@naver.com (H.H.)

² Natural Product Informatics Research Center, Korea Institute of Science and Technology, Gangneung 25451, Korea; nari7040@gmail.com (M.-S.K.); jinsoopark@kist.re.kr (J.-S.P.)

³ Genetic Resources Assessment Division, National Institute of Biological Resources, Incheon 22689, Korea; wjchi76@korea.kr

* Correspondence: sykim01@sunmoon.ac.kr; Tel.: +82-41-530-2390

Abstract: Biorenovation, a microbial enzyme-assisted degradation process of precursor compounds, is an effective approach to unraveling the potential bioactive properties of the derived compounds. In this study, we obtained a new compound, prunetin 4'-O-phosphate (P4P), through the biorenovation of prunetin (PRN), and investigated its anti-inflammatory effects in lipopolysaccharide (LPS)-treated RAW 264.7 macrophage cells. The anti-inflammatory effect of P4P was evaluated by measuring the production of prostaglandin-E₂ (PGE₂), nitric oxide (NO), which is an inflammation-inducing factor, and related cytokines such as tumor necrosis factor- α (TNF α), interleukin-1 β (IL1 β), and interleukin-6 (IL6). The findings demonstrated that P4P was non-toxic to cells, and its inhibition of the secretion of NO—as well as pro-inflammatory cytokines—was concentration-dependent. A simultaneous reduction in the protein expression level of pro-inflammatory proteins such as cyclooxygenase-2 (COX-2) and inducible nitric oxide synthase (iNOS) was observed. Moreover, the phosphorylation of mitogen-activated protein kinases (MAPKs) such as extracellular signal-regulated kinases (ERKs), c-Jun N-terminal kinase (JNK), p38 MAPK (p38), and nuclear factor kappa B (NF κ B) was downregulated. To conclude, we report that biorenovation-based phosphorylation of PRN improved its anti-inflammatory activity. Cell-based in vitro assays further confirmed that P4P could be applied in the development of anti-inflammatory therapeutics.

Keywords: prunetin 4'-O-phosphate; prunetin; anti-inflammatory activities; biorenovation; phosphorylation; MAPK signaling



Citation: Park, T.-J.; Hong, H.; Kim, M.-S.; Park, J.-S.; Chi, W.-J.; Kim, S.-Y. Prunetin 4'-O-Phosphate, a Novel Compound, in RAW 264.7 Macrophages Exerts Anti-Inflammatory Activity via Suppression of MAP Kinases and the NF κ B Pathway. *Molecules* **2021**, *26*, 6841. <https://doi.org/10.3390/molecules26226841>

Academic Editors: Chang-Gu Hyun and Jongsung Lee

Received: 27 September 2021

Accepted: 9 November 2021

Published: 12 November 2021

Publisher's Note: MDPI stays neutral with regard to jurisdictional claims in published maps and institutional affiliations.



Copyright: © 2021 by the authors. Licensee MDPI, Basel, Switzerland. This article is an open access article distributed under the terms and conditions of the Creative Commons Attribution (CC BY) license (<https://creativecommons.org/licenses/by/4.0/>).

1. Introduction

Under hazardous stimuli, for instance, infection and physical injury could trigger an inflammation response [1–3]. In particular, chronic inflammation could be harmful to normal tissues and cause many painful symptoms such as allergy, cardiovascular disease, diabetes, asthma, and cancer [4–6]. Therefore, inhibition of over-expressed inflammation is considered an effective strategy for treating inflammatory diseases [7,8].

Pathogenic bacteria-derived lipopolysaccharide (LPS) can be found on their extracellular surface, the presence of which activates macrophages and, in turn, induces the secretion of cytokines, such as tumor necrosis factor- α (TNF α), interleukin-1 β (IL1 β), and interleukin-6 (IL6) [9–11]. The increased secretion of cytokines promotes the gene and protein expression of inducible nitric oxide synthase (iNOS) and cyclooxygenase-2 (COX-2), as well as their respective end products nitric oxide (NO) and prostaglandin-E₂ (PGE₂) [12,13]. Reportedly, the iNOS-induced excessive expression of NO leads to cell death and disrupts tissue homeostasis [14,15].

Inhibitory κ B (I κ B) is normally bound to NF κ B. During inflammation I κ B kinase (IKK) phosphorylates I κ B, and this allows NF κ B to be released freely [16–18]. Simultaneously, the released NF κ B is rapidly phosphorylated, which enables the translocation of NF κ B to inside the nucleus through the nuclear membrane. DNA promoter-bound NF κ B in turn facilitates the transcription and translation of inflammation-activating genes for COX-2, iNOS, IL6, IL1 β , and TNF α [19,20]. LPS-induced mitogen-activated protein kinases (MAPKs) such as extracellular signal-regulated kinase (ERK), c-Jun N-terminal kinase (JNK), and p38 also play significant roles in NF κ B activation [21–24]. Moreover, via these signaling pathways, transcription factors for the expression of inflammation proteins such as COX-2 and iNOS are activated. Accordingly, MAPKs and NF κ B have been well studied over the development course of potential anti-inflammatory therapeutics. [25–27].

Flavonoids are secondary plant metabolites and are widely contained in fruits, vegetables, and certain drinks [28–30]. In addition, flavonoids are utilized in nutraceutical, pharmaceutical, medicinal, and cosmetic areas [31,32] and have a number of bio-activities, including anti-inflammatory, anti-lipogenic, and anti-cancer effects [33–35]. Flavonoids have a polyphenolic structure and consist of two main groups—2-phenylchromans and the 3-phenylchromans (isoflavones). Isoflavones include genistein, biochanin A, and formononetin, to name a few, and represent a portion of plant-derived secondary metabolites with estrogenic activity; therefore, they are known as phytoestrogens [36,37]. Of these, PRN (7-O-methylgenistein), an O-methylated isoflavone [38], has been shown to inhibit the gene expression and secretion of matrix metalloproteinase-3 (MMP)-3 in chondrocytes [39]. PRN has also been shown to suppress the transcription of obesity genes through a feedback mechanism [40].

Biorenovation facilitates the construction of a drug candidate library with biologically derivative natural compounds. It is a method of microbial enzyme-assisted biodegradation of natural compounds into novel bioactive candidates [41,42]. In our previous study, we showed its efficiency in improving the bioactivity of formononetin 7-O-phosphate derived from formononetin, and 4'-O-isopropyl genistein from genistein [43]. Given the multitude of bioactive properties of PRN, we hypothesized that biorenovation can improve the anti-inflammatory activities of PRN with no significant decrease in cell viability.

Therefore, in this study, we employed biorenovation to derivatize PRN and investigated the anti-inflammatory effects of the derived compound. Here, *Bacillus* sp. JD3-7 was used as a biocatalyst to derivatize PRN, and the biorenovation products were investigated for changes in their chemical structure and anti-inflammatory activities.

2. Results

2.1. Chemical Structures of the Biorenovation Products of PRN

The biorenovation products of PRN (PRBR) using *Bacillus* sp. JD3-7 were detected using high-performance liquid chromatography (HPLC). Two different peaks, excluding PRN, were found in PRBR (Figure 1A).

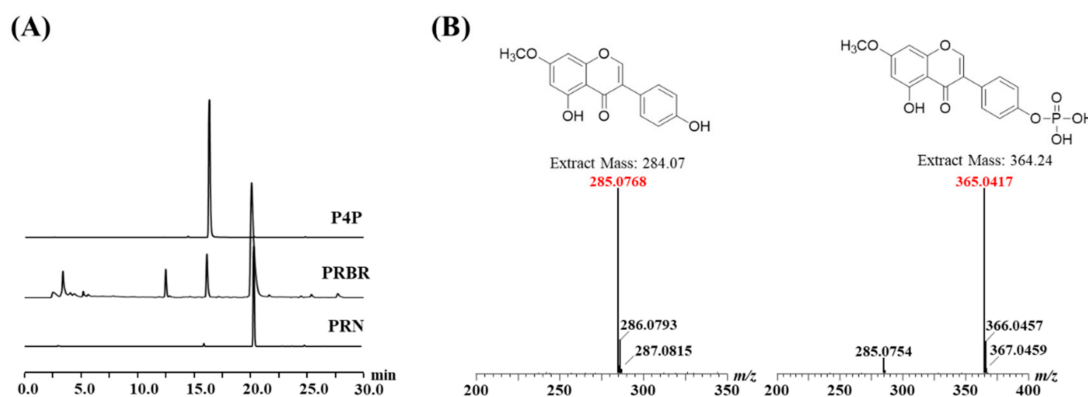


Figure 1. (A) HPLC analysis of prunetin (PRN) and the biorenovation products of prunetin (PRBR) and prunetin 4'-O-phosphate (P4P). (B) Mass analysis of PRN and P4P.

The largest peak among the two, excluding the substrate, was purified using preparative HPLC. Electrospray ionization mass spectrometry (ESI/MS) was employed to ascertain whether the largest peak is a derivative of PRN. As shown in the mass spectrum in Figure 1B, a tallest peak at m/z 285 was identified as that of ionized PRN, and it showed that an $[M + H]^+$ peak at m/z 364 was that of a derivative of PRN. Based on previous studies [44], this result suggests that the hydrogen atom of PRN was phosphorylated by biorenovation.

2.2. NMR Results

The position of phosphorylation was confirmed by NMR experiments. The chemical shifts of H-3' and H-5' (δ_H 7.22 ppm) were downfield-shifted compared to that of prunetin. In addition, C-4' was observed at 152.11 ppm in the ^{13}C -NMR by shielding by phosphorylation. This result indicates phosphorylation at C-4' of prunetin. C-P coupling with J_{C-H} 5.0 Hz caused a split in the carbon signals of C-3' and C-5' (^{13}C -NMR spectrum). Through these results, the position of phosphorylation of P4P was elucidated.

(P4P, 1): 1H -NMR (DMSO- d_6 , 500 MHz): δ 8.40 (1H, s, C-2), 6.42 (1H, s, C-6), 6.68 (1H, s, C-8), 7.53 (2H, d, $J = 3.5$ Hz, C-2', 3'), 7.22 (2H, d, $J = 8.7$ Hz, C-3', 5'), 12.87 (1H, s, C5-OH), and 3.87 (1H, s, C7-OCH₃) (Figure S1, Table S1).

^{13}C -NMR (DMSO- d_6 , 125 MHz): δ 155.62 (C-2), 122.44 (C-3), 180.59 (C-4), 162.16 (C-5), 98.62 (C-6), 165.80 (C-7), 93.05 (C-8), 157.98 (C-9), 105.85 (C-10), 126.54 (C-1'), 130.58 (C-2', 6'), 120.34 (d, $J = 5.2$ Hz, C-3', 5'), 152.11 (C-4'), and 56.62 (C7-CH₃) (Figures S2 and S3, Table S1).

2.3. Effects of P4P on the Viability of RAW 264.7 Cells and NO Production

The RAW 264.7 cells were treated with LPS only or with P4P of 12.5, 25, or 50 μM . As shown in Figure 2A, P4P did not significantly suppress the cells' viability (Figure 2A). Furthermore, the inhibition of NO production was increased as with the increase in the P4P concentration (Figure 2B).

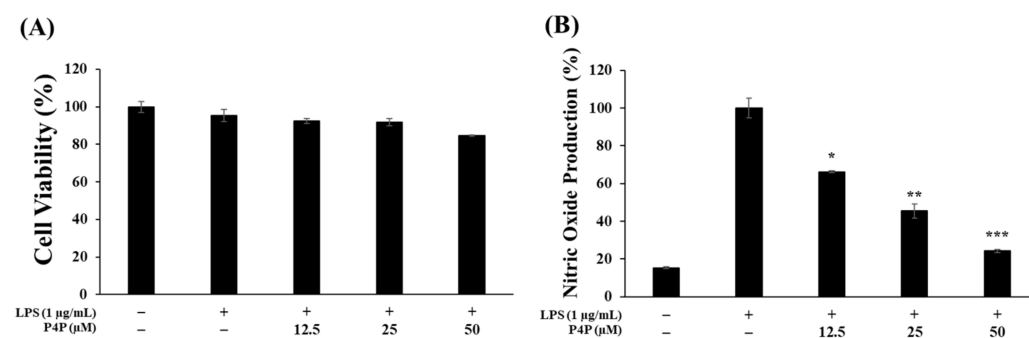


Figure 2. Activities of P4P on the toxicity and production of NO in RAW 264.7 cells induced by LPS. (A) Cells were treated with LPS (1 $\mu g/mL$) in the presence/absence of P4P (0.01% DMSO) for 24 h. (B) The secreted NO level among samples was compared. The values of triplicate experiments are represented as the mean and standard deviation (SD). * $p < 0.05$, ** $p < 0.01$, and *** $p < 0.005$ versus LPS alone.

2.4. Suppression of LPS-Induced IL6, IL1 β , and TNF α Production

The secreted cytokine levels were quantified with an ELISA assay, and their secretion levels among samples were compared. In the P4P-treated samples, IL6 production decreased by 3%, 38%, and 65% with the increase in P4P concentration of 12.5, 25, and 50 μM , respectively (Figure 3A). Similarly, P4P inhibited the expression of TNF α and IL1 β concentration-dependently. Maximal inhibition on the production of IL1 β and TNF α production was achieved at 50 μM of P4P by 43% and 31%, respectively (Figure 3B,C).

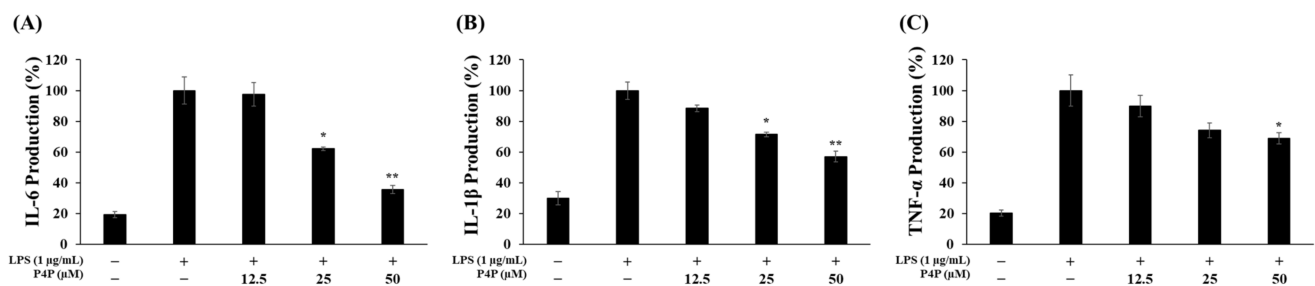


Figure 3. Effect of P4P on the (A) IL6, (B) IL1 β , and (C) TNF α production in LPS-stimulated RAW 264.7 cells. Cell were treated with LPS (1 μ g/mL) in the presence/absence of P4P (0.01% DMSO) for 24 h. Their production was determined by ELISA. The values of triplicate experiments are represented as the mean and standard deviation (SD). * $p < 0.05$ and ** $p < 0.01$ versus LPS alone.

2.5. Suppression of LPS-Induced PGE₂ Secretion and Protein Expression of iNOS and COX-2

LPS-induced PGE₂ production was suppressed by 16%, 37%, and 51% with the increase in P4P concentration of 12.5, 25, and 50 μ M, respectively (Figure 4A).

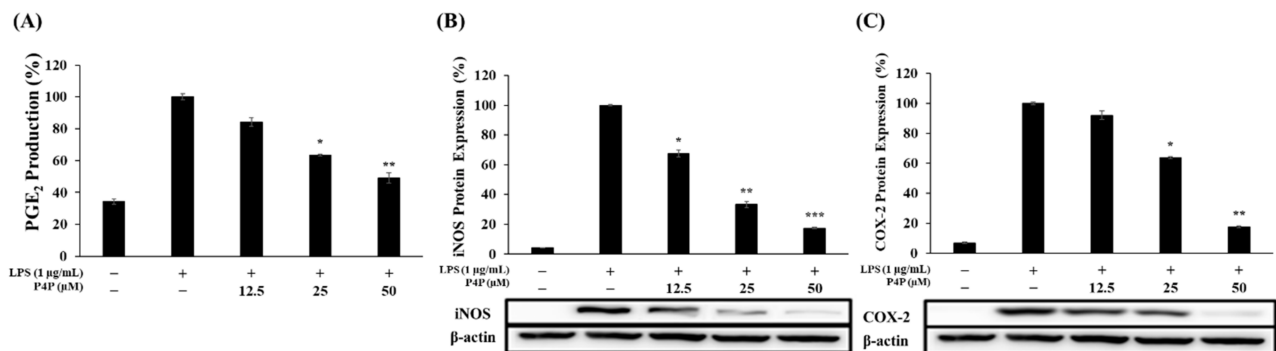


Figure 4. Inhibitory effects of P4P on LPS-induced PGE₂ production and the protein levels of iNOS and COX-2 in RAW 264.7 cells. (A) Cell culture supernatant (100 μ L) of cells stimulated with LPS (1 μ g/mL) in the presence (12.5, 25, and 50 μ M) or absence of P4P (0.01% DMSO) was used to determine the level of PGE₂ production by ELISA. Absorbance was measured at 450 nm. (B,C) The protein levels of iNOS and COX-2 were determined by Western blot. * $p < 0.05$, ** $p < 0.01$, and *** $p < 0.005$ versus LPS alone.

iNOS and COX-2 catalyze the production of NO and PGE₂, respectively. Next, Western blotting was employed to examine the direct involvement of iNOS and COX-2 in their respective catalysis product of NO and PGE₂. The two protein expression levels were significantly suppressed relative to LPS only, and P4P concomitantly decreased the protein levels of COX-2 and iNOS in a concentration-dependent manner. iNOS protein expression relative to LPS only was reduced by 67% and 83% with the increase in P4P concentration of 25 and 50 μ M, respectively (Figure 4B). The reduction in COX-2 protein expression compared to LPS only was respectively decreased by 37% and 83% by P4P at 25 and 50 μ M (Figure 4C). In addition, the iNOS and COX-2 proteins were downregulated to the levels of unstimulated RAW 264.7 cells. These results suggest the simultaneous downregulation of iNOS and COX-2 with their respective reduction in NO and PGE₂ production.

2.6. Expression of Proteins of MAPK and NF κ B Pathways

The presence of LPS in RAW 264.7 activates the MAPK (ERK, JNK, and p38) and NF κ B signaling pathways to boost the production of inflammatory mediators and cytokines [45]. Western blot on the proteins of the MAPK and NF κ B signaling proteins revealed that P4P suppressed the LPS-induced phosphorylation of ERK, JNK, and p38 and was downregulated with the increase in P4P concentration (Figure 5A–C).

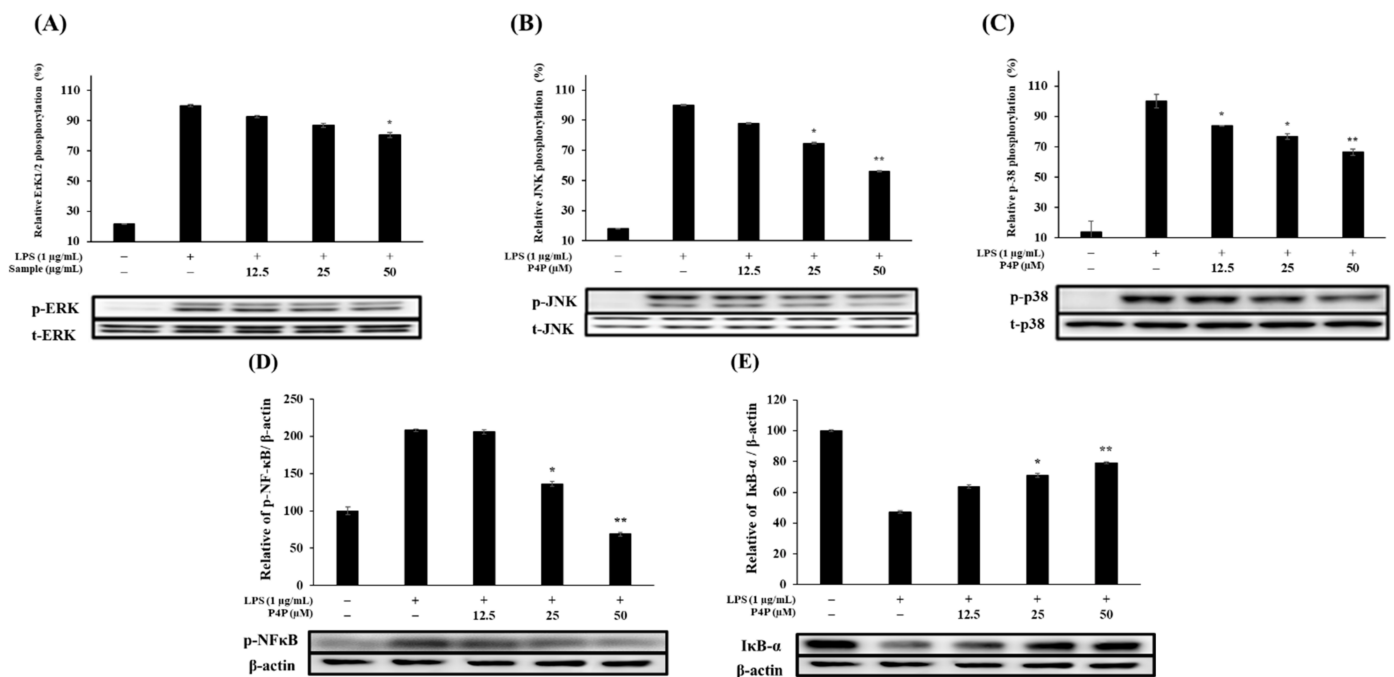


Figure 5. Effects of P4P on mitogen-activated proteins, including (A) ERK, (B) JNK, (C) p38, (D) NFκB, and (E) IκB-kinase activation. Cells were stimulated with LPS (1 μg/mL) in the presence (12.5, 25, or 50 μM) or absence of P4P (0.01% DMSO) for 40 min. the expression levels of MAPK, NFκB, IκB, and β-actin protein were measured. * $p < 0.05$, ** $p < 0.01$ versus LPS alone.

Likewise, phosphorylation of p38 decreased with the increase in P4P concentration (Figure 5C). The results also indicate that P4P treatment decreased the level of NFκB phosphorylation (Figure 5D) while increasing the level of IκB-α expression (Figure 5E). Collectively, P4P exerted its anti-inflammatory properties by the downregulation of the MAPK and NFκB signaling proteins and hindering the secretion of related cytokines and mediators.

3. Discussion

Inflammation is an immune response in vivo that tries to defend the body and repair damaged areas when physical or chemical stimulations are applied to the body. During inflammation, macrophages produce inflammatory mediators (NO and PGE₂) and related cytokines (IL6, IL1β, and TNFα). However, a persistent inflammatory response causes chronic inflammation, which, in turn, can damage body tissues or even lead to cancer [46]. In this respect, studies are being actively performed to find new substances that are active in inhibiting inflammation in order to prevent such chronic inflammation [47–49]. In addition, isoflavones such as genistein, daidzein, glycitein, formononetin, biochanin A, and prunetin are aglycone forms that lack glucose moieties. Recently, these low molecular weight isoflavones have been shown to exhibit diverse pharmacological properties such as anti-inflammatory, anti-oxidant, and anti-tumor effects [50–53]. However, these isoflavones have setbacks such as poor hydrophilicity, which tends to prevent blood-borne drug delivery to inflamed sites and the solubilization of isoflavones in oral care product preparations. Using a high dose of isoflavones is also not recommended [54]. Thus, research to increase the water solubility of isoflavones is currently ongoing [55]. In a previous study, the 7-OH moiety of naringenin was replaced with a phosphate group using biotransformation technology, resulting in a 45-fold increase in the water solubility of naringenin [56]. Accordingly, we employed biorenovation to improve the water solubility of isoflavones. In this study, we performed biorenovation using a known compound, PRN, and confirmed that the chemical structure converted to P4P, a novel compound, using MS and NMR. We then checked whether P4P has anti-inflammatory activity within the non-cytotoxic range, for which MTT and NO production tests were performed. In addition, the secretion levels

of PGE₂ and pro-inflammatory cytokines (IL6, IL1 β , and TNF α), which are representative inflammation markers, were determined using an ELISA kit. Moreover, the protein levels of iNOS and COX-2, their respective catalyst for the production of NO and PGE₂, were investigated through Western blot analysis. Our study confirmed that P4P exhibited its anti-inflammatory activities by the downregulation of inflammation signaling proteins and related cytokines.

The MTT test results confirmed that there was no cytotoxicity within the treated concentrations range (12.5, 25, and 50 μ M), so subsequent experiments were carried out using these concentrations (Figure 2A). To determine whether P4P inhibits the production of inflammatory mediators at the following concentrations, RAW 264.7 macrophages were treated with LPS only or along with P4P sample treatments. As shown in Figures 2B and 4A, both NO and PGE₂ production were dramatically increased upon LPS treatment but were significantly decreased with an increasing concentration of P4P. In addition, we performed Western blot experiments to determine whether the reduction in these inflammatory mediators was regulated by the reduction in iNOS and COX-2 protein expression. As a result, the significantly attenuated expression of iNOS and COX-2 by P4P treatment was confirmed (Figure 4). Based on these results, it was confirmed that P4P treatment in LPS-stimulated macrophages downregulates both the protein expression of iNOS and COX-2 and their respective catalysis products NO and PGE₂.

It has been reported that macrophages stimulated by LPS activate the initial inflammatory response by stimulating the production of pro-inflammatory cytokines [57]. Therefore, the effect of P4P on the expression of inflammation-related cytokines was evaluated with ELISA assays. As shown in Figure 3, it was confirmed that compared to LPS, only the level of cytokines (IL6, IL1 β , and TNF α) was decreased with the increase in P4P concentrations.

The MAPK and NF κ B signaling pathways are well-known in the regulation of the inflammatory response. Various harmful stimuli, such as LPS, ultraviolet rays, and chromosomal damaging substances, induce the activation of MAPK proteins (ERK, JNK, and p38) through their phosphorylation, which ultimately directly increases the production and expression of inflammation-related mediators and cytokines such as TNF α and IL1 β . In addition, ERK is involved in signaling pathways that promote cell growth or differentiation [58–60]. To evaluate the inhibitory effect of P4P on the phosphorylation of the MAPK family, Western blot analysis was performed. The results showed that the significant downregulation of the LPS-induced phosphorylation of ERK, JNK, and p38 was observed with the increase in P4P concentration.

The NF κ B signaling pathway is known to regulate the expression of iNOS and COX-2. The complex form of NF κ B and I κ B- α normally exists in the cytoplasm, but during an inflammatory response, NF κ B phosphorylation and I κ B- α degradation are promoted. In addition, phosphorylated NF κ B translocates to inside nucleus, forming complexes with DNA promoters, increasing the transcription of inflammation-related genes such as for iNOS and COX-2, thereby promoting an inflammatory response [61,62]. Therefore, to confirm whether P4P affects phosphorylation in the NF κ B signaling pathway, immunoblotting was conducted. The immunoblotting data show that P4P inhibited NF κ B phosphorylation and I κ B- α degradation in a concentration-dependent manner. Our mechanistic studies also suggest that P4P downregulated the expression of pro-inflammatory mediators and cytokines via the downregulation of the MAPK and NF κ B signaling pathways.

In summary, this is the first time that biorenovation has been shown to modify the structure of PRN and to generate P4P with anti-inflammatory properties and increased aqueous solubility. The experimental results of LPS-treated RAW 264.7 macrophages show that P4P exerted the downregulation of inflammation in LPS-stimulated macrophages via the downregulation of the MAPK and NF κ B signaling proteins. The water solubility of P4P is expected to increase, and our *in vitro* assays further confirmed that this could be utilized in the development anti-inflammatory therapeutics.

4. Materials and Methods

4.1. Chemical Preparation

Prunetin (PRN), trifluoroacetic acid (TFA), acetone, 3-(4,5-dimethylthiazol-2-yl)-2,5-diphenyltetrazolium bromide (MTT), dimethyl sulfoxide (DMSO), Griess reagent (1% *w/v* sulfanilamide, 0.1% *w/v* *N*-(1-naphthyl)ethylene diamine hydrochloride, 2.5% *v/v* phosphoric acid), rabbit anti-mouse IgG antibody, and horseradish peroxidase (HRP) conjugate were purchased from Sigma-Aldrich (St. Louis, MO, USA). Nutrient broth containing peptones and beef extract was purchased from Oxoid (Waltham, MA, USA). The PG buffer (phosphate glycerin buffer) contained 2% *v/v* glycerin, 50 mM sodium phosphate, pH 7.2. Dulbecco's modified eagle medium (DMEM), fetal bovine serum (FBS), a mixture of penicillin and streptomycin, and phosphate-buffered saline (PBS) were purchased from Gibco (Thermo Fisher Scientific, Inc., Waltham, MA, USA). FBS was inactivated at 56 °C for 30 min. DMEM was mixed with a heat-inactivated FBS (10% *v/v*) and antibiotics mixture (1% *v/v*). Skim milk was purchased from Becton (Dickinson & Co., Sparks, MD, USA).

4.2. Biorenovation of PRN

The strain used in the biorenovation was *Bacillus* sp. JD3-7 from the Korean Agricultural Culture Collection (designated number 92346P, KACC, Wanju, KOR). *B.* sp. JD3-7 was cultured in nutrient broth containing peptones and beef extract at 30 °C for 18 h. Afterward, the strains were pelleted by spin-down (4416 g, 15 min, 4 °C) to remove the supernatant, excluding pellets. The remaining cell culture media were completely washed out twice with PG buffer. Subsequently, PRN was cultured with PG buffer and *Bacillus* sp. JD3-7 microbes were added. The biorenovation was performed at 30 °C and 200 rpm for 72 h. Afterward, the biorenovation reaction was centrifuged at 4416 × *g* for 10 min, and the debris-free liquid phase was freeze-dried.

4.3. HPLC Analysis and Purification of PRN Derivatives

High performance liquid chromatography (HPLC; Shimadzu, Shimadzu Scientific Instruments, Inc., Baltimore, DC, USA) was used to purify and analyze the PRN derivatives. HPLC consisting of a 3200 digital UV-VIS detector, controller, and Shim-Pack GIS C18, 5 μm, 250 × 4.6 mm I.D. (227-30106-08, Shimadzu Scientific Instruments, Inc., Baltimore, DC, USA). The column oven temperature was maintained at 40 °C. The binary solvent system consisted of (A) water with 0.1% *v/v* trifluoroacetic acid (TFA) and (B) acetonitrile (ACN), with a linear gradient of (B) 10%–100% ACN for 30 min. The PRN derivatives and PRN were injected at a 10 μL injection volume with a 1 mL/min flow rate.

4.4. LCMS and NMR Analysis

To decide the molecular weight of P4P and PRN, high-resolution quadrupole-time-of-flight electrospray ionization–mass spectrometry (HR-QTOF ESI-MS) consisting of UPLC coupled with a SYNAPT G2-Si column was achieved in positive ion mode. Using mass data analysis software, MassLynx ver. 4.1 (Waters Corporation, Milford, MA, USA), the masses for the PRN biorenovation products were extracted from the mass data and matched with the previously determined masses for the phosphorylated form of PRN. NMR spectra were obtained using an NMRS 500 NMR (Agilent Technology, Santa Clara, CA, USA) spectrometer with the residual solvent peaks (DMSO-*d*₆ = δH 2.50) of the deuterated NMR solvents as the reference peaks.

4.5. Cell Maintenance and Cytotoxicity Assays

RAW 264.7, mouse macrophage cell line (KCLB, Seoul, Korea), were cultured in DMEM (Gibco, Thermo Fisher Scientific, Inc., Waltham, MA, USA) supplemented with 10% *v/v* heat-inactivated fetal bovine serum (FBS; Gibco, Thermo Fisher Scientific, Inc., Waltham, MA, USA) and 1% *v/v* penicillin and streptomycin (Gibco, Thermo Fisher Scientific, Inc., Waltham, MA, USA). The cells were cultured in 18 cm² culture plates (SPL Life Sciences Co., Ltd., Pocheon, Korea) at a density of 1 × 10⁶ cells/plate, maintained

in a humidified environment at 37 °C and 5% CO₂, and passaged every three days at approximately 70%–80% confluence to avoid overgrowth. Cells were seeded in 0.47 cm² culture plates (Thermo Fisher Inc., Waltham, MA, USA) at a density of 8 × 10⁴ cells/well. LPS (1 µg/mL) alone and in combination with three different P4P concentrations of 12.5, 25, and 50 µM were added to each well at the same time and cultured for another 24 h. The level of cell detachment off the plate was quantified using MTT reagent [63]. The cells were incubated at a final concentration of 1 mg mL⁻¹ of MTT in culture medium for 4 h in a CO₂ incubator (Thermo Fisher Inc., Waltham, MA, USA) and then the spent culture medium was removed and washed twice in PBS. The insoluble form of formazan crystals was dissolved in DMSO, and its absorbance was determined on a microplate spectrophotometer (Multiskan GO, Thermo Fisher Inc., Waltham, MA, USA) at a 570 nm wavelength.

4.6. Quantification of NO and PGE₂ Secretion

As described in Section 4.4., macrophages were stimulated with LPS (1 µg/mL) only or in combination with P4P (12.5, 25, or 50 µM) and further incubated another 24 h. The cultured cell supernatant (100 µL) was mixed with an equal volume of Griess reagent and incubated at room temperature for 10 min, and absorbance was measured at 540 nm to measure NO production [64,65]. PGE₂ ELISA kits were purchased from R&D Systems (Minneapolis, MN, USA). In each case, sample measurements were performed in duplicate. The optical density was determined on a microplate spectrophotometer using a 450 nm wavelength.

4.7. Determination of IL6, IL1β, and TNFα Production

As described in Section 4.4., three concentrations of P4P (12.5, 25, and 50 µM) with or without LPS (1 µg/mL) were treated in macrophage cells. The inhibitory effect of P4P on the secretion of pro-inflammatory cytokines (IL6, IL1β, and TNFα) in the culture suspension was determined by ELISA kits, such as Mouse IL6 (Becton, Dickinson and Company, Sparks, MD, USA), Mouse IL1β/IL1F2 (R&D Systems, Minneapolis, MN, USA), and Mouse TNF alpha (Invitrogen, Carlsbad, CA, USA).

4.8. Immunoblotting

Immunoblotting was carried out as per the method of Kocic et al. [66]. RAW 264.7 cells were lysed in RIPA buffer (Bio-Rad, Hercules, CA, USA) containing protease inhibitor. A Bradford assay kit (Pierce BCA Protein Assay Kit, Thermo Scientific, Waltham, MA, USA) was used to quantify the extracted proteins. After protein molecular weight (20 µg)-based separation by 10% SDS-PAGE, the resultant gel was blotted to 0.45 µm polyvinylidene difluoride (PVDF) membranes (Bio-Rad, Hercules, CA, USA) using the Trans-Blot Turbo system (Bio-Rad, Hercules, CA, USA). The blotted membranes were then blocked with 10% *w/v* skim milk for 2 h and washed four times with TBST (Tween 20-added TBS at 0.05% *v/v*). Afterward, the membranes were incubated overnight at 4 °C with primary antibodies such as COX-2, iNOS, Phospho-Erk1/2 (Thr202/Tyr204), Phospho-p38 (Thr180/Tyr182), Phospho-SAPK/JNK (Thr183/Tyr185), p44/42 MAPK, p38, SAPK/JNK, Phospho-NFκB p65 (Ser536) (93H1), and IκB-α (L35A5). Then, the membranes were conjugated with secondary antibody (rabbit anti-mouse IgG antibody) at room temperature for 2 h, and the antibody-bound proteins on the membranes were visualized using enhanced chemiluminescence reagent (ECL) (Bio-Rad, Hercules, CA, USA). Additionally, the presence and intensity of the target protein on a membrane were measured using ImageQuant 1.3 (LAS4000 mini, GE Healthcare Japan Corp., Tokyo, Japan).

4.9. Statistical Analyses

The measured values are represented as the mean ± standard deviation. Statistically significant differences between means were uncovered using unpaired Student's *t*-tests (95% confidence).

Supplementary Materials: The following are available online, Figure S1: ^1H -NMR spectra of prunetin 4'-O-phosphate (P4P, 1); Figure S2: ^{13}C -NMR spectra of prunetin 4'-O-phosphate (P4P, 1); Figure S3: HMBC correlation of prunetin 4'-O-phosphate (P4P, 1); Table S1: ^1H and ^{13}C -NMR chemical shifts of prunetin 4'-O-phosphate (P4P, 1).

Author Contributions: Conceptualization, S.-Y.K. and W.-J.C.; formal analysis, T.-J.P., M.-S.K. and J.-S.P.; data curation, T.-J.P., M.-S.K. and H.H.; writing—original draft preparation, T.-J.P.; writing—review and editing, S.-Y.K. and W.-J.C.; supervision, S.-Y.K.; project administration, S.-Y.K. All authors have read and agreed to the published version of the manuscript.

Funding: This research was supported by a grant from the National Institute of Biological Resources (NIBR), funded by the Ministry of Environment (MOE) of the Korea (NIBR202102109). This work was also supported by an intramural grant (2Z06482) from the Korea Institute of Science and Technology, Korea.

Institutional Review Board Statement: Not applicable.

Informed Consent Statement: Not applicable.

Data Availability Statement: Not applicable.

Conflicts of Interest: The authors declare no conflicts of interest.

Sample Availability: Samples of the compounds aren't available from the authors.

References

1. Kim, Y.-J.; Kim, H.-J.; Lee, J.Y.; Kim, D.-H.; Kang, M.S.; Park, W. Anti-Inflammatory Effect of Baicalein on Polyinosinic–Polycytidylic Acid-Induced RAW 264.7 Mouse Macrophages. *Viruses* **2018**, *10*, 224. [[CrossRef](#)] [[PubMed](#)]
2. Murray, P.J.; Wynn, T.A. Protective and pathogenic functions of macrophage subsets. *Nat. Rev. Immunol.* **2011**, *11*, 723–737. [[CrossRef](#)] [[PubMed](#)]
3. Lin, W.W.; Karin, M. A cytokine-mediated link between innate immunity, inflammation, and cancer. *J. Clin. Investig.* **2007**, *117*, 1175–1183. [[CrossRef](#)]
4. Ryu, H.W.; Lee, S.U.; Lee, S.; Song, H.-H.; Son, T.H.; Kim, Y.-U.; Yuk, H.J.; Ro, H.; Lee, C.-K.; Hong, S.-T.; et al. 3-Methoxy-catalposide inhibits inflammatory effects in lipopolysaccharide-stimulated RAW264.7 macrophages. *Cytokine* **2017**, *91*, 57–64. [[CrossRef](#)] [[PubMed](#)]
5. Guha, M.; Mackman, N. LPS induction of gene expression in human monocytes. *Cell. Signal.* **2001**, *13*, 85–94. [[CrossRef](#)]
6. Moretta, A.; Marcenaro, E.; Sivori, S.; Della Chiesa, M.; Vitale, M.; Moretta, L. Early liaisons between cells of the innate immune system in inflamed peripheral tissues. *Trends Immunol.* **2005**, *26*, 668–675. [[CrossRef](#)]
7. Dai, G.-F.; Zhao, J.; Jiang, Z.-W.; Zhu, L.-P.; Xu, H.-W.; Ma, W.-Y.; Chen, X.-R.; Dong, R.-J.; Li, W.-Y.; Liu, H.-M. Anti-inflammatory effect of novel andrographolide derivatives through inhibition of NO and PGE2 production. *Int. Immunopharmacol.* **2011**, *11*, 2144–2149. [[CrossRef](#)]
8. Kaminska, B. MAPK signalling pathways as molecular targets for anti-inflammatory therapy—From molecular mechanisms to therapeutic benefits. *Biochim. Biophys. Acta (BBA)-Prot. Proteom.* **2005**, *1754*, 253–262. [[CrossRef](#)]
9. Tsai, T.-C.; Tung, Y.-T.; Kuo, Y.-H.; Liao, J.-W.; Tsai, H.-C.; Chong, K.-Y.; Chen, H.-L.; Chen, C.-M. Anti-inflammatory effects of *Andrographis camphorata*, a herbal medicine, in a mouse skin ischemia model. *J. Ethnopharmacol.* **2015**, *159*, 113–121. [[CrossRef](#)]
10. Wang, W.; Jenkinson, C.; Griscavage, J.; Kern, R.; Arabolos, N.; Byrns, R.; Cederbaum, S.; Ignarro, L. Co-induction of Arginase and Nitric Oxide Synthase in Murine Macrophages Activated by Lipopolysaccharide. *Biochem. Biophys. Res. Commun.* **1995**, *210*, 1009–1016. [[CrossRef](#)]
11. Zhu, F.; Du, B.; Xu, B. Anti-inflammatory effects of phytochemicals from fruits, vegetables, and food legumes: A review. *Crit. Rev. Food Sci. Nutr.* **2018**, *58*, 1260–1270. [[CrossRef](#)] [[PubMed](#)]
12. Shimizu, T.; Shibuya, N.; Narukawa, Y.; Oshima, N.; Hada, N.; Kiuchi, F. Synergistic effect of baicalein, wogonin and oroxylin A mixture: multistep inhibition of the NF κ B signaling pathway contributes to an anti-inflammatory effect of *Scutellaria root* flavonoids. *J. Nat. Med.* **2018**, *72*, 181–191. [[CrossRef](#)]
13. Pearson, G.; Robinson, F.; Beers Gibson, T.; Xu, B.-E.; Karandikar, M.; Berman, K.; Cobb, M.H. Mitogen-Activated Protein (MAP) Kinase Pathways: Regulation and Physiological Functions*. *Endocr. Rev.* **2001**, *22*, 153–183. [[CrossRef](#)] [[PubMed](#)]
14. Hommes, D.W.; Peppelenbosch, M.P.; van Deventer, S.J. Mitogen activated protein (MAP) kinase signal transduction pathways and novel anti-inflammatory targets. *Gut* **2003**, *52*, 144–151. [[CrossRef](#)]
15. Lieb, K.; Engels, S.; Fiebich, B.L. Inhibition of LPS-induced iNOS and NO synthesis in primary rat microglial cells. *Neurochem. Int.* **2003**, *42*, 131–137. [[CrossRef](#)]
16. Makarov, S.S. NF- κ B as a therapeutic target in chronic inflammation: recent advances. *Mol. Med. Today* **2000**, *6*, 441–448. [[CrossRef](#)]

17. Koo, H.J.; Yoon, W.J.; Sohn, E.H.; Ham, Y.M.; Jang, S.A.; Kwon, J.E.; Jeong, Y.J.; Kwak, J.H.; Sohn, E.; Park, S.Y.; et al. The analgesic and anti-inflammatory effects of *Litsea japonica* fruit are mediated via suppression of NF κ B and JNK/p38 MAPK activation. *Int. Immunopharmacol.* **2014**, *22*, 84–97. [[CrossRef](#)]
18. Kiemer, A.K.; Hartung, T.; Huber, C.; Vollmar, A.M. Phyllanthus amarus has anti-inflammatory potential by inhibition of iNOS, COX-2, and cytokines via the NF κ B pathway. *J. Hepatol.* **2003**, *38*, 289–297. [[CrossRef](#)]
19. Wang, D.; DuBois, R.N. The role of COX-2 in intestinal inflammation and colorectal cancer. *Oncogene* **2009**, *29*, 781–788. [[CrossRef](#)]
20. Park, K.E.; Qin, Y.; Bavry, A. Nonsteroidal anti-inflammatory drugs and their effects in the elderly. *Aging Health* **2012**, *8*, 167–177. [[CrossRef](#)]
21. Kim, Y.-S.; Ahn, C.-B.; Je, J.-Y. Anti-inflammatory action of high molecular weight *Mytilus edulis* hydrolysates fraction in LPS-induced RAW264.7 macrophage via NF- κ B and MAPK pathways. *Food Chem.* **2016**, *202*, 9–14. [[CrossRef](#)] [[PubMed](#)]
22. Shalini, V.; Pushpan, C.K.; Sindhu, G.; Jayalekshmy, A.; Helen, A. Tricin, flavonoid from *Njavara* reduces inflammatory responses in hPBMCs by modulating the p38MAPK and PI3K/Akt pathways and prevents inflammation associated endothelial dysfunction in HUVECs. *Immunobiology* **2016**, *221*, 137–144. [[CrossRef](#)] [[PubMed](#)]
23. Zhang, T.-T.; Wang, M.; Yang, L.; Jiang, J.-G.; Zhao, J.-W.; Zhu, W. Flavonoid glycosides from *Rubus chingii* Hu fruits display anti-inflammatory activity through suppressing MAPKs activation in macrophages. *J. Funct. Foods* **2015**, *18*, 235–243. [[CrossRef](#)]
24. Li, D.; Chen, J.; Ye, J.; Zhai, X.; Song, J.; Jiang, C.; Wang, J.; Zhang, H.; Jia, X.; Zhu, F. Anti-inflammatory effect of the six compounds isolated from *Nuclea officinalis* Pierre ex Pitard, and molecular mechanism of strictosamide via suppressing the NF κ B and MAPK signaling pathway in LPS-induced RAW 264.7 macrophages. *J. Ethnopharmacol.* **2017**, *196*, 66–74. [[CrossRef](#)]
25. Pateras, I.; Giaginis, C.; Tsigris, C.; Patsouris, E.; Theocharis, S.; Madonna, R.; De Caterina, R. NF- κ B signaling at the crossroads of inflammation and atherogenesis: searching for new therapeutic links relevance of new drug discovery to reduce NF- κ B activation in cardiovascular disease. *Expert Opin. Ther. Targets* **2014**, *18*, 1089–1101. [[CrossRef](#)]
26. Maulik, N.; Sato, M.; Price, B.D.; Das, D.K. An essential role of NF- κ B in tyrosine kinase signaling of p38 MAP kinase regulation of myocardial adaptation to ischemia. *FEBS Lett.* **1998**, *429*, 365–369. [[CrossRef](#)]
27. Bonizzi, G.; Karin, M. The two NF- κ B activation pathways and their role in innate and adaptive immunity. *Trends Immunol.* **2004**, *25*, 280–288. [[CrossRef](#)]
28. Castañeda-Ovando, A.; de Lourdes Pacheco-Hernández, M.; Páez-Hernández, M.E.; Rodríguez, J.A.; Galán-Vidal, C.A. Chemical studies of anthocyanins: a review. *Food Chem.* **2009**, *113*, 859–871. [[CrossRef](#)]
29. Burak, M.; Imen, Y. Antioxidant properties of flavonoids. *Med. J. Indones.* **1999**, *19*, 296–304.
30. Lee, Y.K.; Yuk, D.Y.; Lee, J.W.; Lee, S.Y.; Ha, T.Y.; Oh, K.W.; Yun, Y.P.; Hong, J.T. Epigallocatechin-3-gallate prevents lipopolysaccharide-induced elevation of β -amyloid generation and memory deficiency. *Brain Res.* **2009**, *1250*, 164–174. [[CrossRef](#)]
31. Walker, E.H.; Pacold, M.E.; Perisic, O.; Stephens, L.; Hawkins, P.; Wymann, M.; Williams, R.L. Structural Determinants of Phosphoinositide 3-Kinase Inhibition by Wortmannin, LY294002, Quercetin, Myricetin, and Staurosporine. *Mol. Cell* **2000**, *6*, 909–919. [[CrossRef](#)]
32. Metodiewa, D.; Kochman, A.; Karolczak, S. Evidence for antiradical and antioxidant properties of four biologically active N, N, diethylaminoethyl ethers of flavanone oximes: a comparison with natural polyphenolic flavonoid (rutin) action. *Biochem. Mol. Biol. Int.* **1997**, *41*, 1067–1075. [[PubMed](#)]
33. Hayashi, T.; Sawa, K.; Kawasaki, M.; Arisawa, M.; Shimizu, M.; Morita, N. Inhibition of Cow's Milk Xanthine Oxidase by Flavonoids. *J. Nat. Prod.* **1988**, *51*, 345–348. [[CrossRef](#)]
34. Silver, L.L.; Bostian, K. Screening of natural products for antimicrobial agents. *Eur. J. Clin. Microbiol. Infect. Dis.* **1990**, *9*, 455–461. [[CrossRef](#)]
35. Grange, J.M.; Davey, R.W. Antibacterial properties of propolis (bee glue). *J. R. Soc. Med.* **1990**, *83*, 159–160. [[CrossRef](#)] [[PubMed](#)]
36. Shriner, R.L.; Hull, C.J. Isoflavones. III. The Structure of Prunetin and a New Synthesis of Genistein¹. *J. Org. Chem.* **1945**, *10*, 288–291. [[CrossRef](#)]
37. Middleton, E., Jr.; Kandaswami, C.; Theoharides, T.C. The effects of plant flavonoids on mammalian cells: implications for inflammation, heart disease, and cancer. *Pharmacol. Rev.* **2000**, *52*, 673–751.
38. Barnes, S. Soy isoflavones—phytoestrogens and what else? *J. Nutr.* **2004**, *134*, 1225S–1228S. [[CrossRef](#)]
39. Nam, D.C.; Kim, B.K.; Lee, H.J.; Shin, H.D.; Lee, C.J.; Hwang, S.C. Effects of prunetin on the proteolytic activity, secretion and gene expression of MMP-3 in vitro and production of MMP-3 in vivo. *Korean J. Physiol. Pharmacol.* **2016**, *20*, 221–228. [[CrossRef](#)] [[PubMed](#)]
40. Ahn, T.-G.; Yang, G.; Lee, H.-M.; Kim, M.-D.; Choi, H.-Y.; Park, K.-S.; Lee, S.-D.; Kook, Y.-B.; An, H.-J. Molecular mechanisms underlying the anti-obesity potential of prunetin, an O-methylated isoflavone. *Biochem. Pharmacol.* **2013**, *85*, 1525–1533. [[CrossRef](#)] [[PubMed](#)]
41. Koirala, M.; Lee, Y.K.; Kim, M.S.; Chung, Y.C.; Park, J.S.; Kim, S.Y. Biotransformation of Naringenin by *Bacillus amyloliquefaciens* Into Three Naringenin Derivatives. *Nat. Prod. Commun.* **2019**, *14*, 1934578–19851971.
42. Kim, K.-M.; Park, J.-S.; Choi, H.; Kim, M.-S.; Seo, J.-H.; Pandey, R.P.; Kim, J.W.; Hyun, C.-G.; Kim, S.-Y. Biosynthesis of novel daidzein derivatives using *Bacillus amyloliquefaciens* whole cells. *Biocatal. Biotransform.* **2018**, *36*, 469–475. [[CrossRef](#)]
43. Choi, H.; Park, J.-S.; Kim, K.-M.; Kim, M.; Ko, K.-W.; Hyun, C.-G.; Ahn, J.W.; Seo, J.-H.; Kim, S.-Y. Enhancing the antimicrobial effect of genistein by biotransformation in microbial system. *J. Ind. Eng. Chem.* **2018**, *63*, 255–261. [[CrossRef](#)]

44. Kim, M.S.; Park, J.S.; Chung, Y.C.; Jang, S.C.; Hyun, C.G.; Kim, S.Y. Anti-Inflammatory Effects of Formononetin 7-O-phosphate, a Novel Biorenovation Product, on LPS-Stimulated RAW 264.7 Macrophage Cells. *Molecules* **2019**, *24*, 3910. [[CrossRef](#)]
45. Dong, N.; Li, X.; Xue, C.; Zhang, L.; Wang, C.; Xu, X.; Shan, A.; Dong, N.; Li, X.; Xue, C.; et al. Astragalus polysaccharides alleviates LPS-induced inflammation via the NF- κ B/MAPK signaling pathway. *J. Cell Physiol.* **2020**, *235*, 5525–5540. [[CrossRef](#)] [[PubMed](#)]
46. Kim, E.K.; Choi, E.-J. Compromised MAPK signaling in human diseases: an update. *Arch. Toxicol.* **2015**, *89*, 867–882. [[CrossRef](#)]
47. Dhillon, A.S.; Hagan, S.; Rath, O.; Kolch, W. MAP kinase signalling pathways in cancer. *Oncogene* **2007**, *26*, 3279–3290. [[CrossRef](#)]
48. Fuentes, E.; Rojas, A.; Palomo, I. NF- κ B signaling pathway as target for antiplatelet activity. *Blood Rev.* **2016**, *30*, 309–315. [[CrossRef](#)] [[PubMed](#)]
49. Dinarello, C.A. Anti-inflammatory Agents: Present and Future. *Cell* **2010**, *140*, 935–950. [[CrossRef](#)]
50. Mazumder MA, R.; Hongsprabhas, P. Genistein as antioxidant and antibrowning agents in in vivo and in vitro: A review. *Biomed. Pharmacother.* **2016**, *82*, 379–392. [[CrossRef](#)]
51. Li, Q.-S.; Li, C.-Y.; Li, Z.-L.; Zhu, H.-L. Genistein and its Synthetic Analogs as Anticancer Agents. *Anti-Cancer Agents Med. Chem.* **2012**, *12*, 271–281. [[CrossRef](#)] [[PubMed](#)]
52. Luo, L.; Zhou, J.; Zhao, H.; Fan, M.; Gao, W. The anti-inflammatory effects of formononetin and ononin on lipopolysaccharide-induced zebrafish models based on lipidomics and targeted transcriptomics. *Metabolomics* **2019**, *15*, 153. [[CrossRef](#)] [[PubMed](#)]
53. Li, J.; Van Valkenburgh, J.; Hong, X.; Conti, P.S.; Zhang, X.; Chen, K. Small molecules as theranostic agents in cancer immunology. *Theranostics* **2019**, *9*, 7849–7871. [[CrossRef](#)]
54. Tang, L.; Singh, R.; Liu, Z.; Hu, M. Structure and Concentration Changes Affect Characterization of UGT Isoform-Specific Metabolism of Isoflavones. *Mol. Pharm.* **2009**, *6*, 1466–1482. [[CrossRef](#)]
55. Zhao, J.; Yang, J.; Xie, Y. Improvement strategies for the oral bioavailability of poorly water-soluble flavonoids: An overview. *Int. J. Pharm.* **2019**, *570*, 118642. [[CrossRef](#)] [[PubMed](#)]
56. Zhang, S.; Li, D.D.; Zeng, F.; Zhu, Z.H.; Song, P.; Zhao, M.; Duan, J.A. Efficient biosynthesis, analysis, solubility and anti-bacterial activities of succinylglycosylated naringenin. *Nat. Prod. Res.* **2019**, *33*, 1756–1760. [[CrossRef](#)]
57. Byun, S.H.; Yang, C.H.; Kim, S.C. Inhibitory effect of Scrophulariae Radix extract on TNF α , IL1 β , IL6 and Nitric Oxide production in lipopolysaccharide-activated Raw 264.7 cells. *Korea J. Herbol.* **2005**, *20*, 7–16.
58. Hyun, M.S.; Woo, W.H.; Hur, J.M.; Kim, D.H.; Moon, Y.J. The role of ROS and p38 MAP kinase in berberine-induced apoptosis on human hepatoma HepG2 cells. *J. Korean Soc. Appl. Biol. Chem.* **2008**, *51*, 129–135.
59. Ahn, J.Y.; Lee, E.R.; Kim, J.Y.; Cho, S.G. Protein phosphorylation as a regulatory mechanism of various cellular function. *Cancer Prev. Res.* **2006**, *11*, 1–8.
60. Chun, J.H.; Kang, S.; Varani, J.; Lin, J.; Fisher, G.J.; Voorhees, J.J. Decreased extracellular signal regulated kinase and increased stress activated MAP kinase activities in aged human skin in vitro. *J. Investig. Dermatol.* **2000**, *15*, 177–182. [[CrossRef](#)]
61. Liden, J.; Rafter, I.; Truss, M.; Gustafsson, J.A.; Okret, S. Glucocorticoid effects on NF- κ B binding in the transcription of the ICAM-1 gene. *Biochem. Biophys. Res. Commun.* **2000**, *273*, 1008–1014. [[CrossRef](#)]
62. Pruett, S.B.; Fan, R.; Zheng, Q. Characterization of glucocorticoid receptor translocation, cytoplasmic I κ B, nuclear NF- κ B, and activation of NF- κ B in T lymphocytes exposed to stress-inducible concentrations of corticosterone in vivo. *Int. Immunopharmacol.* **2003**, *3*, 1–16. [[CrossRef](#)]
63. Kumar, P.; Nagarajan, A.; Uchil, P. Analysis of Cell Viability by the MTT Assay. *Cold Spring Harb. Protoc.* **2018**, *2018*, pdb-prot095505. [[CrossRef](#)] [[PubMed](#)]
64. Kamada, T.; Kang, M.-C.; Phan, C.-S.; Zani, I.I.; Jeon, Y.-J.; Vairappan, C.S. Bioactive Cembranoids from the Soft Coral Genus *Simularia* sp. in Borneo. *Mar. Drugs* **2018**, *16*, 99. [[CrossRef](#)]
65. Rho, H.S.; Ghimeray, A.K.; Yoo, D.S.; Ahn, S.M.; Kwon, S.S.; Lee, K.H.; Cho, D.H.; Cho, J.Y. Kaempferol and Kaempferol Rhamnosides with Depigmenting and Anti-Inflammatory Properties. *Molecules* **2011**, *16*, 3338–3344. [[CrossRef](#)]
66. Kocić, J.; Santibañez, J.F.; Krstić, A.; Mojsilović, S.; Ilić, V.; Bugarski, D. Interleukin-17 modulates myoblast cell migration by inhibiting urokinase type plasminogen activator expression through p38 mitogen-activated protein kinase. *Int. J. Biochem. Cell Biol.* **2013**, *45*, 464–475. [[CrossRef](#)] [[PubMed](#)]